STUDY OF HYDROGEN EMBRITTLEMENT AND DETERMINATION OF E110 FUEL CLADDING MECHANICAL PROPERTIES BY RING COMPRESSION TESTING

Hygreeva Kiran NAMBURI [1], Luca OTTAZZI [2], Michal CHOCHOLOUSEK [1], Jakub KREJCI [3]

[1]*Centrum výzkumu Řež s. r. o., Husinec-Řež, Czech Republic, EU, nab@cvrez.cz*

[2]*Department of Mechanical Engineering, University of Genoa, Italy, EU*

[3]*UJP PRAHA a.s., Praha - Zbraslav, Czech Republice, EU*

Abstract

Zirconium based alloys are commonly used as material for fuel claddings in the light water reactors. Claddings act as first metallic barriers against loss of fission products during the nuclear power plant operation, intermittent storage or final dry storage. During the reactor operation, claddings are subjected to different stress levels at high temperatures as well as neutron radiation. This results in their corrosion, hydrogen diffusion, hydrogen embrittlement and creep. The integrity of claddings is always critical issue for during reactor operation, loss of coolant accidents and during storage of spent fuel. In this work, ring compression testing method developed was applied to study hydrogen embrittlement, to evaluate the stress-strain behavior and hoop fracture properties of E110 (Zr-based) fuel claddings. Tests were performed on un-irradiated fuel claddings with varying hydrogen concentrations 0, 189, 217, 328 and 393 wt. ppm at 380 °C. Further the stress - strain curves were calculated and mathematical models were used to determine the collapse load and ultimate tensile strength. The results show that the collapse load and the tensile strength values depend strongly on hydrogen concentration. In particular, tensile strength experiment data shows significant change in its trend after reaching the maximum hydrogen solubility limit at 380 °C. Furthermore RCT method showed to be simple-effective, removes complexity of specimen preparation, reduce the amount of radioactive waste and reproducible for evaluating the strength and embrittlement of irradiated claddings in hot cells at varying conditions.

Keywords: Metallurgy, steel, properties, applications, testing methods

1. INTRODUCTION

Zirconium based fuel claddings serve as barrier between the pellets and the fuel rod environment, avoiding the release of fuel or fission products during service into the reactor core or cooling system or after service into storage containments. Zirconium and its alloys have a significant property, a very low neutron absorption cross section, 30 times less than iron. This is the main reason for the selection of zirconium and its alloys as core materials to obtain better neutron efficiency in thermal reactors. In addition, zirconium alloys also possess good corrosion resistance, mechanical strength and are relatively resistant to radiation damage [1-2]. During the reactor operation, claddings accumulate hydrogen due to oxidation and are subjected to degradation resulting from their exposure to high temperature, high pressure and irradiation. When the hydrogen content in zirconium alloys exceeds the terminal solid solubility limit, diffused hydrogen atoms react with the zirconium matrix and formation of zirconium hydrides occurs [3]. The content of the absorbed hydrogen into the cladding tubes depends on many factors and is part of today's research work. In any case, the amount of hydrogen increases with the increase in the fuel burn-up. Hence hydrogen content is an increasing quantity with respect to reactor cycles [4]. Possible degradation mechanisms of fuel claddings include [6]: creep [5], hydrogen embrittlement (reduction in ductility) [7] and Delayed Hydride Cracking [8, 9] etc.

Figure 1 shows the phase diagram of the binary Zr-H system. Different phases of zirconium hydrides are visible. The δ-zirconium hydride phase has a face centered cubic structure ($ZrH_{1.66}$), γ-hydride phase has a

body centered tetragonal structure (ZrH) and ε-hydride phase has a face centered tetragonal structure (ZrH_2). δ- and ε-hydrides are the two stable hydride phases in the form of platelets, while the γ-hydrides are the metastable hydrides in the form of needles. ε-hydrides are observed at very high hydrogen contents and γ-hydrides are formed in quenched specimens [3]. After the usage of fuel assemblies for a period of time in nuclear reactor, they are firstly sent to the wet storage in water for heat decay and then sent to final disposal, called dry storage. Initial temperatures at the dry storage are higher than wet storage as the specific heats of cooling media are lower than water. Under these situations at specific conditions (internal pressure, temperature, hydrogen content) creep [10], hydride re-orientation [11-12] and related effects at spent fuel dry storage [13-15] are the most likely degradation mechanisms that could cause failure in fuel claddings. Therefore the study on mechanical integrity of the fuel cladding tubes is very important.

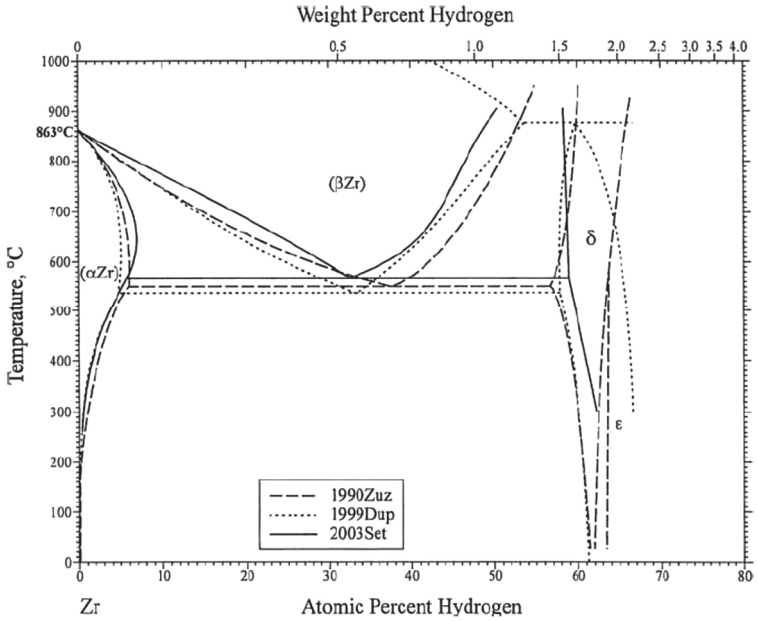

Figure 1 Phase diagram of binary Zr-H system, detail of the (αZr) phase region [3]

When the hydrogen solubility limit in these zirconium based cladding alloys is exceeded (see **Figure 1**), their excess amount results in the formation of zirconium hydride precipitates. These precipitates have been shown to be less ductile than the surrounding zirconium alloy matrix, so can have deleterious effects on the mechanical properties. It has been demonstrated that these hydrides may embrittle the cladding and reduce its mechanical properties. The resulting embrittlement depends on the concentration and geometrical distribution of the hydrides. The hydrides which adopt a radial orientation in the cladding, may reduce the fracture properties of the cladding more the ones that adopt a hoop orientation [16], on particular the orientation affect the ductile to brittle transition temperature (DBTT) [17-19].

Traditionally the ring tensile test is one of the most used to calculate the stress-strain curve in the hoop direction. The initial test consisted on applying a force from the inner surface of the sample cladding sample by means of two half cylinders. The ring tensile test presents two important experimental difficulties: the samples need a relatively complex matching (important factor when the test is performed with irradiated samples) and the results are affected by some parameters difficult to measure, such as the friction factor and the gap between the sample and the load device. Alternatively, the ring compression test could be employed to obtain the stress-strain plastic curve. It is the easiest and simplest methodology in the future mechanical properties, especially for cladding materials embrittlement experiment in the hot cell. By means of the RCT (Ring Compression Test), there is no need to consider the influence of friction between testing devices and

samples. Besides this, the sample preparation would be more concise, this is important for preparing the irradiated samples.

Current study is focused on evaluating the mechanical properties in the hoop direction of the zirconium cladding E110 with different hydrogen contents 0 (as received), 189, 217, 328, 393 wt. ppm, was investigated through the use of the RCT at 380 °C and determining the best practices for testing irradiated claddings in hot-cells to perform cladding embrittlement studies.

2. MATERIALS AND EXPERIMENTS

2.1. Materials and specimens dimensions

Specimen examined in this study was fabricated of the E110 alloy of tubular section, 10 mm long with outer diameter of ~ 9.1 mm and wall thickness of ~ 570 μm provided by UJP Prague. The chemical composition of E110 cladding tube was 99 % Zr and 1 % Nb with minor impurities of Fe and O. Cladding sections were pre-hydrogenated in autoclave to desired hydrogen contents (0, 189, 217, 328, 393 wt. ppm) with outer diameter app. 9.15 mm and specimen length 10-12 mm.

2.2. Experimentation

2.2.1. Metallography and microstructure

Metallography was performed before mechanical testing, to determine the hydrogen content and hydrides distribution in pre-hydrogenated specimens. The samples were embedded into the cold epoxy resin. First half section of the samples was embedded in the tubes Axial Direction (AD) and the second half section was embedded in Circumferential Direction (CD) as is represented in **Figure 2**. Mechanical grinding was performed on the grinding polishing machine LaboPol-25 with grinding paper. Followed by fine polish where diamond suspensions (3 μm and 1μm particle size) and colloidal silica suspension (0.04 μm) were used. The samples for Optical microscopy analysis were prepared by etching them in a solution of 100 ml H_2O_2, 4.5 ml HNO_3 and 0.5 -1 ml HF, to inspect the hydride distribution in the cladding.

2.2.2. Mechanical testing

Ring Compression Test was selected in the present study in order to obtain the mechanical properties of tubular sample. The lengths of tubular sample were choose to had a plane strain state during compression process (length > outer diameter). The samples with different amount of hydrogen (0, 189, 217, 328, 393 wt. ppm) were tested at 380 °C. To check the reproducibility, RCT was repeated 2 times for each condition (just once for 0 and 393 ppm).

Mechanical tests were performed with the strength testing device Z250 from Zwick with a strength range up to 250 kN, in the corresponding furnace, as shown in **Figure 3**. The first sample with 0 ppm was initially fastened by 10 N pre-load at the centre between two rigid flats, the other samples (189, 217, 328, 393 ppm) weren't fastened at the upper flat (no pre-load), because we wanted to avoid the compression before the application of the testing load. Then with the heating rate of 20 °C/min the sample was heated from room temperature to 380 °C. Test matrix is given in **Table 1**.

In order to make a homogeneous distribution of the hydrogen within, the sample was left 30 min after set temperature, before the load application. Afterwards the movable upper flat crush the sample on the fixed lower flat with a 0.5 mm/min load-line displacement rate. The compression system operated within a furnace, in which three thermocouples (above, below and near the sample) were inserted to ensure that the target temperature was achieved during the test as shown in **Figure 4**. Outer oxide layer thickness was about 5 μm not enough to have a macroscopic influence in the sample behavior.

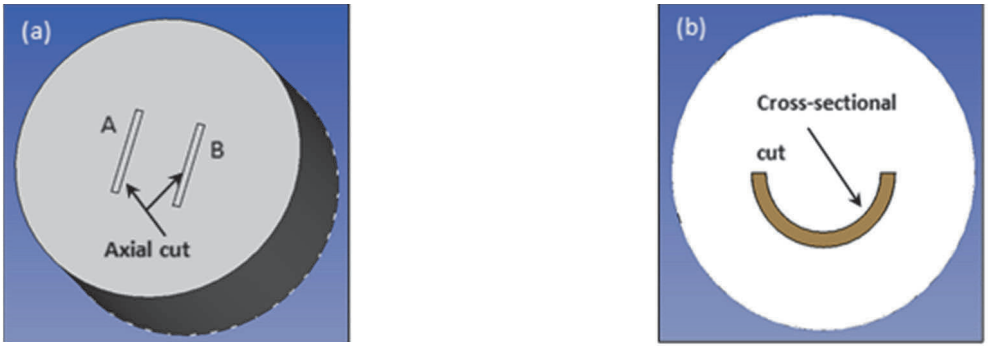

Figure 2 Sectioned sample embedding in an epoxy resin (a) in the axial / longitudinal direction, (b) in transverse direction

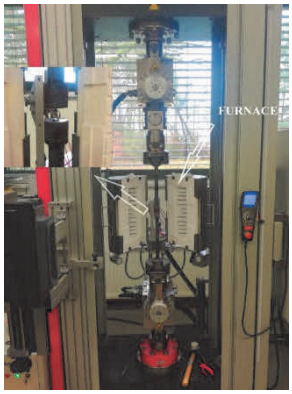

Figure 3 Ring Compression Testing machine with furnace and compression heads

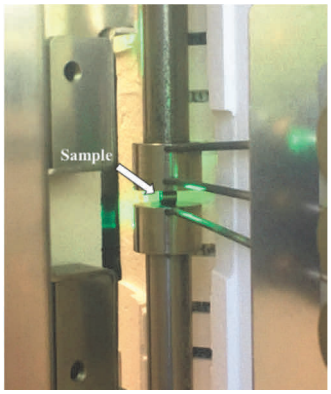

Figure 4 Thermocouples inserted into furnace close to specimen during the RCT test

Table 1 Specimen test matrix for ring compression testing to study hydrogen embrittlement in E110 fuel claddings

Number of specimens	H content (ppm)	Test Temperature (°C)	Length of specimen (mm)
1	0	380	9.91
2	189	380	12.28 & 11.62
2	217	380	9.99 &10.51
2	328	380	10.35 & 9.92
1	393	380	10.24

3. RESULTS AND DISCUSSION

3.1. Microstructural investigations

Transverse (cross-sectional) and longitudinal metallographic images from the pre-hydrogenated specimens are shown in **Figure 5**. A uniform layer of oxide thickness is evident, which was formed during autoclave oxidation process. Optical examination of the hydrogenated metallographic specimens revealed the presence of hydride platelets aligned in circumferential direction. These are called circumferential hydrides formed on the circumferential-longitudinal planes and were in the form of long chains. In both regions, the average length of macro-hydrides in the longitudinal direction was 150 ± 1.2 μm and in the circumferential direction was 182 ± 8 μm. Grains and grain boundaries are however not discernible optically, and thus, we cannot obtain any detailed information regarding location of the hydrides with respect to the grains and grain boundaries.

Figure 6 shows the 3D re-construction of the observed hydrides on the circumferential-longitudinal plane. In this figure, on the right side is shown the habit planes of the circumferential hydrides in hexagonal zirconium lattice.

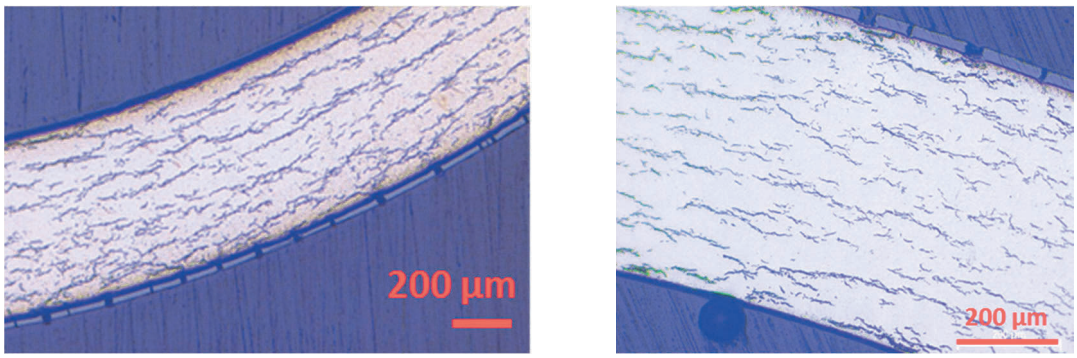

Figure 5 Hydrides oriented in the radial-circumferential orthographic plane

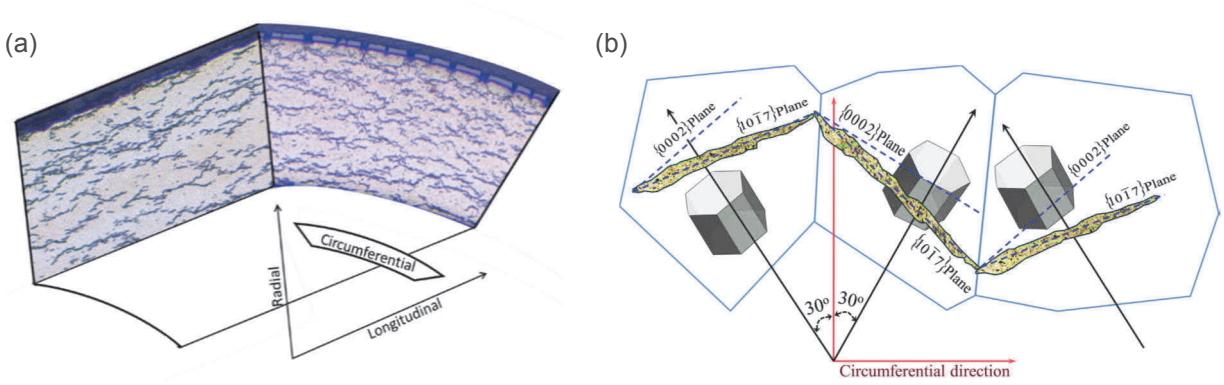

Figure 6 (a) 3D reconstruction of hydrides orientation in the creep tested hydrided E110 cladding and (b) schematic of hydride formation on habit plane [20]

3.2. Mechanical investigations

The load - displacement curves obtained from ring compression testing at various levels of hydrogen content tested at 380 °C are shown in **Figure 7**. On the recorded load-time curve, three areas was highlight to show the macroscopic behaviour of the sample during RCT at 380 °C. **Figure 8** represents the deformation stages of cladding during the ring compression test with varying loading at constant temperature. Initially there was a linear relationship between the stress and the plastic strain with a slope practically vertical. In this area the sample (at the macroscopic level), didn't show significant shape difference compared to the original sample. The next stage, known as plastic deformation zone, takes place from the elbow to the huge change of slope. In this area, differently from other studies at room temperature [21], the maximum and the minimum didn't appeared. This because at this temperature the maximum strain reached at ring equatorial azimuth remains lower than the failure strain. Then the larger deformation took place, the vertical diameter of the sample decreased gently until the contact between the upper and lower face, then the load continued to increase until the force reaches the 5 kN of load.

During RCT, it is known that sample underwent plastic deformation after initial elastic deformation. As shown in **Figure 9**, the collapse force P_0, where large plastic deformation occurred, can be obtained directly from the load-displacement curve by getting the intersection of the lines extended from elastic and plastic region, respectively. After extracting collapse force from the load-displacement curve, one of targeted properties of the material, Ultimate Tensile Stress (UTS), could be estimated by the equations provided from previous works

[22], which were based on some theoretical models of plastic theory and several basic mechanical theories. Thus, the dimensions of sample as in **Figure 10**, including outer radius *R*, thickness *t* and length *L*, act as important factors in these equations which aim to convert collapse force into UTS.

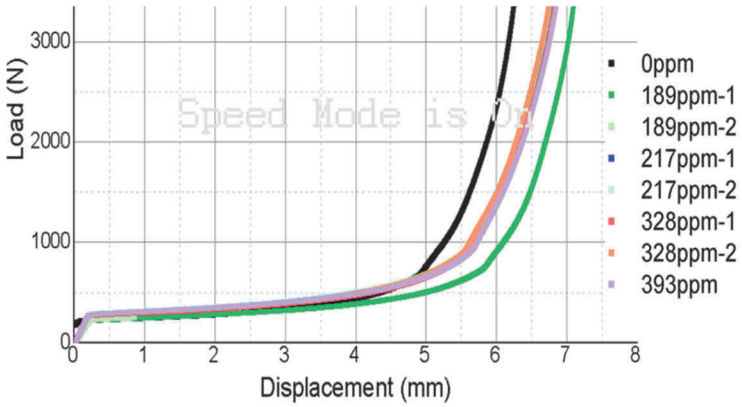

Figure 7 Load-displacement curves from RCT tests with different hydrogen concentration at 380 °C

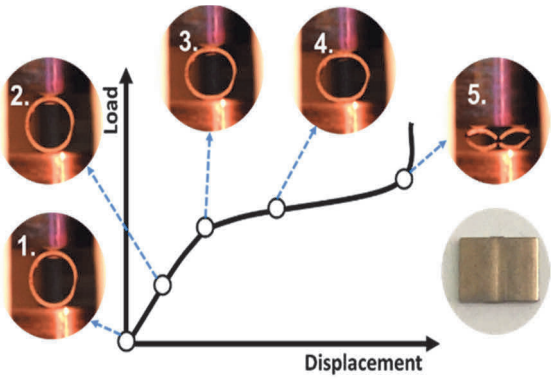

Figure 8 Stages of cladding tube deformation during the ring compression testing

Due to the complexity of the stress distribution in the sample, the ring is assumed to be perfectly plastic, which means no working hardening occurred in the whole process of RCT. With the plastic theory, the correlation between collapse stress σ_0 and plastic moment M_p can be obtained by

$$M_p = 1/4\ \sigma_0\ t^2\ L \quad (1)$$

where M_p is defined as the moment, at which the entire cross section is under its yield stress. Furthermore, based on the law of conservation of energy, the external virtual work done by P_0 is known to equal the internal virtual work done by M_p. Thus, the collapse force can be defined as

$$P_0 = (4\ M_p) / R = (\sigma_0\ t^2\ L) / R \quad (2)$$

For working hardening material, a similar correlation can also be established and be used to get the collapse stress σ_0, as shown below:

$$\sigma_0 = \alpha\ P_0\ R / (t^2\ L) \quad (3)$$

Note that the constant α equals 0.866 in this work because the value of α depends upon the lengths of sample. α equals 0.866 when the sample is in a plane strain state (longer than one diameter) in contrast to 1 in the plane stress state($L < 5\ t$). Besides, the influence of the testing temperatures can be considered to be included in the natural definition of collapse force, so these all equations are appropriate to be used in present study. Collapse stress is calculated from RCT, and then can be linearly correlated to the UTS of tensile test through the following coefficients

$R_m = \sigma_0 / K_{UTS}$ (4)

The load-displacement curves obtained from the RCT as shown in **Figure 9** basically demonstrated two different main types of results. Increasing the hydrogen concentration, it is possible to see that the samples with 189 wt. ppm H_2 without hydrides have the point of contact between the upper and lower face (where there is the huge change of slope) higher than the other concentration (the sample with 0 ppm was already deformed due to the initial pre-load). This indicates that the samples with a higher hydrogen concentration were less ductile, due to the precipitation of δ-hydrides in the sample. Moreover ring compression tests shown that, at this relatively high temperature, the hydrides cannot act as a crack initiation site. We can suppose that zirconium metal matrix, may regain enough ductility to accommodate the large plastic deformation even with the precipitated hydrides.

The tests developed from room temperature to the set temperature of 380 °C, showed different tensile strength for different hydrogen condition as in **Figure 11**. After the hydrogen composition with 189 wt. ppm H_2, the change of the trend indicated that between the 189 wt. ppm and 217 wt. ppm hydrogen concentration, the hydrogen solubility limit had been reached. As shown in **Figure 12**, the maximum solubility of hydrogen in zirconium at 380 °C is more or less 215 wt. ppm. In the test performed with 189 wt. ppm H_2 the whole amount of hydrogen presented in the sample was dissolved in the α-Zr. On the other hand, when the hydrogen concentration was higher, the excess amount of hydrogen precipitated and formed the δ-zirconium hydride. This stable phase has a different density and lattice structure and dimensions which can cause the hydrogen-embrittlement behavior. The tensile strengths R_m, which could be obtained by converting the collapse loads with **Eqs. (3) & (4)** are summarized in **Table 2**.

Table 2 Tensile strength (R_m) at the test temperature 380 °C with different hydrogen content

Number of specimens	**H content** (wt. ppm)	**Tensile strength** (MPa)
1	0	236.9
2	189	193.6 & 207.04
2	217	293.3 & 270.47
2	328	287.97 & 271.41
1	393	287.39

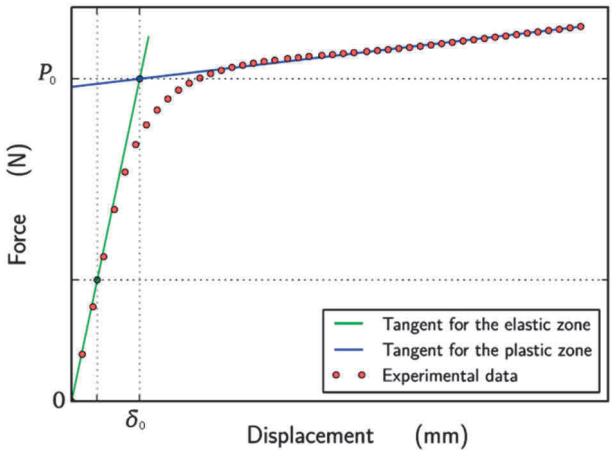

Figure 9 Load-displacement curve of ring compression test

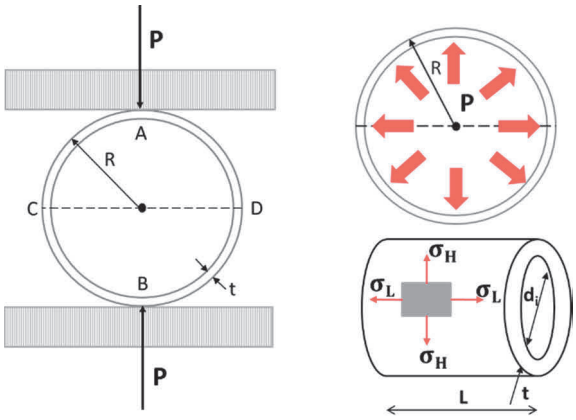

Figure 10 Schematic of test specimen during ring compression testing

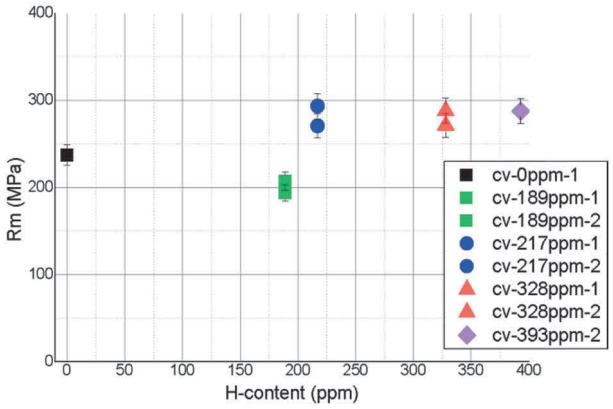

Figure 11 Tensile strength at 380 °C with different hydrogen concentrations

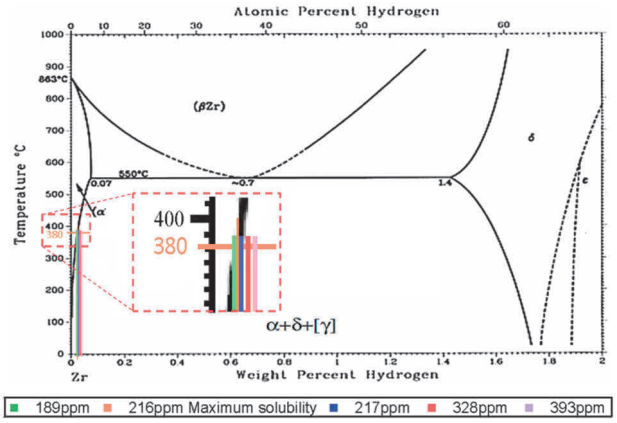

Figure 12 Binary Zr-H phase diagram

4. CONCLUSIONS

- Ring Compression Test is an interesting test method to determine some useful mechanical proprieties in hoop direction of tube-shape materials. Its cost-reducing and the low material consumption gave the test a real potential.
- The zirconium alloy E110 in full recrystallized condition showed that at this temperature and with these hydrogen concentrations, the hydrides can't act as a crack initiation site.
- The experimental results showed that this test is very sensitive to low hydrogen concentration. For only 328 wt. ppm of hydrogen, a remarkable effect in the collapse load is produce.
- The presence of δ-hydrides in the samples causes an increase of tensile strength due to the presence of harder (always more brittle) particles within the microstructure.

ACKNOWLEDGEMENTS

This work has been partially supported by the ENEN+ project that has received funding from the Euratom research and training Work Programme 2016 - 2017 - 1 #755576.

The presented work was financially supported by the Ministry of Education, Youth and Sport Czech Republic - project LQ1603 Research for SUSEN. This work has been realized within the SUSEN Project (established in the framework of the European Regional Development Fund (ERDF) in project CZ.1.05/2.1.00/03.0108 and of the European Strategy Forum on Research Infrastructures (ESFRI) in the project CZ.02.1.01/0.0/0.0/15_008/0000293, which is financially supported by the Ministry of Education, Youth and Sports - project LM2015093 Infrastructure SUSEN

REFERENCES

[1] LEMAIGNAN, C. and MOTTA, Arthur T. Zirconium Alloys in Nuclear Applications. *Materials Science and Technology: A Comprehensive Treatment*, Nuclear Materials, B, B. R. T. Frost, Ed., New York, VCH, 1994. vol. 10, pp. 1-51.

[2] RUDY, Konings. Zirconium Alloys: Properties and Characteristics. *Comprehensive Nuclear Materials*. 2012, vol. 2, pp. 217-232.

[3] OKAMOTO, H. H-Zr (Hydrogen-Zirconium). *Journal of Phase Equilibria and Diffusion*. 2006. no. 27, pp. 548-549.

[4] KOOK, D. Review of spent fuel integrity evaluation for dry storage. *Nuclear Engineering and Technology*. 2013. vol. 45, no. 1, pp. 115-124.

[5] ALAM, T. A review on the clad failure studies. *Nuclear Engineering and Design*. 2011. pp. 3658- 3677.

[6] SUMAN, S. Hydrogen in Zircaloy: Mechanism and its impacts. *International Journal of Hydrogen Energy*. 2015. pp. 5976 - 5994.

[7] FERIA, F. and HERRANZ, L.E. Creep assessment of Zry-4 cladded high burnup fuel under dry storage. *Progress in Nuclear Energy*. 2011. pp. 395-400.

[8] SINGH, R.N. Stress-reorientation of hydrides and hydride embrittlement of Zr-2.5 wt% Nb pressure tube alloy. *Journal of Nuclear Materials*. 2004. no. 325, pp. 26-33.

[9] NAMBURI, Hygreeva K., VALANCE, K. S. and BERTSCH, J. Delayed hydride cracking in Zircaloy-2 fuel cladding tubes. *Top Fuel Reactor Fuel Performance*. 2012.

[10] KIM, Y. S. Precipitation of reoriented hydrides and texture change of α-zirconium grains during delayed hydride cracking of Zr-2.5Nb pressure tube. *Journal of Nuclear Materials*. 2001. no. 297, pp. 292-302.

[11] SINGH, R. N. Influence of temperature on threshold stress for reorientation of hydrides and residual stress variation across thickness of Zr-2.5Nb alloy pressure tube. *Journal of Nuclear Materials.* 2006. no. 359, pp. 208-219. KESE, K. Hydride re-orientation in Zircaloy and its effect on the tensile properties. Stockholm: SKI report 98:32, 1998. p. 49.

[12] KIM, Hyun-Gil. The effects of creep and hydride on spent fuel integrity during interim dry storage. *Nuclear Engineering and Technology*. 2010. vol. 42, no. 3, pp. 249-258.

[13] JOE R. Albert M. Threat of hydride re-orientation to spent fuel integrity during transportation accidents: Myth or reality? In *Proceedings of the 2007 International LWR Fuel Performance Meeting*. 2007. San Francisco. pp. 464-471.

[14] CHA, Hyun-Jin. The effect of hydrogen and oxygen contents on hydride reorientations of zirconium alloy cladding tubes. *Nuclear Engineering Technology*. 2015. no. 147, pp. 746-755.

[15] ARSENE, S. and BAI, J. B. *Effet de la microstructure et de la temperature sur la transition ductile-fragile des Zircaloy hydrurés*. PhD dissertation, Ecole Centrale Paris, 1997.

[16] PARRY, G. W. and EVANS W. Occurrence of ductile hydrides in zircaloy-2. *Nucleonics*. 1964. no. 22, p. 65.

[17] Wallace, A. C., Shek, G. K. and Lepik, O. E. Effect of hydride morphology on Zr-2.5Nb fracture toughness. Zirconium in the nuclear industry. *ASTM Spec. Tech. Publ*. 1989. no. 1023, pp. 66-88

[18] LINGA, K., CHARIT, I. Texture development and anisotropic deformation of Zircaloys. *Progress in Nuclear Energy*. 2006. no. 48, pp. 325-359.

[19] SUMAN, S. Hydrogen in Zircaloy: Mechanism and its impacts. *International Journal of Hydrogen Energy*. 2015. no. 40, pp. 5976 - 5994.

[20] BUSSER, Vincent, BAIETTO-DUBOURG, Marie-Christine, DESQUINES, Jean DURIEZ, Christian and MARDON, Jean-Paul. Mechanical response of oxidized Zircaloy-4 cladding material submitted to a ring compression test. *Journal of Nuclear Material*. 2009. no. 384, pp. 87-95.

[21] REDDY, Yella T. and REID, S. R. On obtaining material properties from the ring compression test. *Nuclear Engineering and Design*. 1979. no. 52, pp. 257-263.

[22] NEMAT-ALLA, Mahmoud. Reproducing hoop stress-strain behavior for tubular material using lateral compression test. *International Journal of Mechanical Sciences*. 2003. no. 45, pp. 605-621